# Phase-space curvature in spin-orbit-coupled ultracold atomic systems

J. Armaitis,[*] J. Ruseckas,[†] and E. Anisimovas[‡]

*Institute of Theoretical Physics and Astronomy, Vilnius University, Saulėtekio Ave. 3, LT-10222 Vilnius, Lithuania*
(Received 10 February 2017; published 17 April 2017)

We consider a system with spin-orbit coupling and derive equations of motion which include the effects of Berry curvatures. We apply these equations to investigate the dynamics of particles with equal Rashba-Dresselhaus spin-orbit coupling in one dimension. In our derivation, the adiabatic transformation is performed first and leads to quantum Heisenberg equations of motion for momentum and position operators. These equations explicitly contain position-space, momentum-space, and phase-space Berry curvature terms. Subsequently, we perform the semiclassical approximation and obtain the semiclassical equations of motion. Taking the low-Berry-curvature limit results in equations that can be directly compared to previous results for the motion of wave packets. Finally, we show that in the semiclassical regime, the effective mass of the equal Rashba-Dresselhaus spin-orbit-coupled system can be viewed as a direct effect of the phase-space Berry curvature.

## I. INTRODUCTION

The geometrical concept of curvature has found multiple applications in various branches of physics [1], including the general theory of relativity [2], gauge theories in particle physics [3], and, most recently, condensed-matter physics in the guise of Berry curvatures [4]. In simple terms, position-space Berry curvature can be understood as a result of magnetization texture in real space, while momentum-space Berry curvature requires spin-orbit coupling (SOC) [4,5]. Here, SOC is understood in the broad sense, i.e., as linking the velocity to some quantized internal characteristic of the particle.

Even though SOC arises naturally in crystals that lack an inversion center, that is not the case in ultracold-atom systems [6]. There, the coupling between the motion of each neutral atom and its hyperfine spin [7] (or other degrees of freedom [8,9]) has to be artificially engineered [10]. Recently, this field has seen considerable progress [11–13], and some of the proposed spin-orbit-coupling schemes have been experimentally realized. In particular, one-dimensional equal Rashba-Dresselhaus [14,15] SOC was implemented several years ago [16] and has received a substantial amount of attention [17]. Furthermore, there has been promising experimental progress in engineering two-dimensional Rashba SOC [18,19], while three-dimensional Weyl SOC remains an active theoretical research direction [20–23]. Most of this work is concentrated on utilizing the internal states of the atom and transitions between them with no spatial dependence. However, other means, such as spatial degrees of freedom and periodic driving of the system, can also be efficiently exploited for similar purposes [24–26]. For example, it is possible to achieve strong effective magnetic field in optical lattices and thus simulate various condensed-matter Hamiltonians [27–32]. According to the concept of synthetic dimensions [33], internal degrees of freedom can be used to emulate additional spatial directions [7,8,33–37]. In this context, coupling between spatial and internal degrees of freedom was demonstrated using both hyperfine [7] and long-lived electronic [8,9] states. Central to understanding all of these advances is the notion of the Berry phase [38].

The Berry phase, as well as Berry curvatures in real and momentum spaces, has been thoroughly discussed in the literature in various contexts (see [4,12] and references therein). However, up to now considerably less attention has been paid to phase-space Berry curvatures, especially outside the solid-state physics community. It was only recently realized that this phase-space Berry curvature can lead to an alternation of the density of states [39,40]. This change in the density of states might in turn be used to detect topological objects, such as skyrmions, by a mundane electrical measurement. This turns out to be particularly relevant to solid-state materials, where both spin-orbit coupling and magnetization textures are present [41,42].

Theoretical progress concerning phase-space Berry curvature has been mostly concentrated on lattice systems in the semiclassical approximation. In an early publication [43], wave-packet propagation in a slowly perturbed crystal was described using a combined Hamiltonian-Lagrangian approach. A derivation of the equations of motion using the Ehrenfest theorem without the Lagrangian formalism was presented in Ref. [44]. A series of articles by Gosselin and coworkers developed a purely Hamiltonian semiclassical treatment [45–47] and also perturbatively addressed the problem beyond the semiclassical (lowest order in the reduced Planck constant $\hbar$) approximation [48,49]. In other work, quantum kinetic equations were derived for multiband systems, taking the effects of phase-space Berry curvature into account [50].

In this paper we approach the phase-space Berry curvature with applications in ultracold-atom systems in mind. We present two main results. First, we derive quantum-mechanical Heisenberg equations of motion, where various Berry curvatures show up without relying on the semiclassical approximation [Eqs. (28)]. These equations also allow us to recover the semiclassical results of Ref. [43] by explicitly taking the small-curvature limit purely within the Hamiltonian formalism. Second, we show that in the experimentally accessible equal Rashba-Dresselhaus spin-orbit-coupled system, the effective mass in the semiclassical single-minimum regime

---

[*]jogundas.armaitis@tfai.vu.lt
[†]julius.ruseckas@tfai.vu.lt
[‡]egidijus.anisimovas@ff.vu.lt
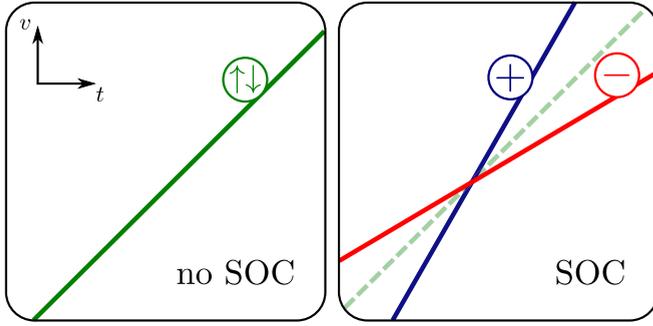
FIG. 1. In the absence of spin-orbit coupling both spin species ($\uparrow$ and $\downarrow$) respond to a spin-independent linear potential in the same way since their masses are equal (left). When the spin-orbit coupling is turned on, adiabatic motion occurs in dispersion branches labeled by $+$ and $-$. The effective mass in the two branches is different, resulting in a different response to the same potential (right). This effect can be explained by the phase-space Berry curvature in the semiclassical regime (see Sec. VI for more details).

can be reinterpreted as the phase-space Berry curvature (see Fig. 1).

This paper is organized as follows. In Sec. II we present the problem and introduce the notation. In Sec. III we attack the general problem by performing an adiabatic approximation, which results in the Heisenberg equations of motion. To show that this treatment is also of practical interest, we then apply these results to two particular cases in Sec. IV. Namely, we derive the (quantum) equations of motion when either the position-space Berry curvature or the momentum-space Berry curvature is nonvanishing. In Sec. V, we perform the semiclassical approximation for the general problem and obtain the corresponding equations of motion with various Berry-curvature terms explicitly shown. We investigate the experimentally relevant equal Rashba-Dresselhaus Hamiltonian in our framework in Sec. VI. Finally, Sec. VII summarizes our results and provides some directions for future work.

## II. POSITION-DEPENDENT SPIN-ORBIT COUPLING

Let us consider the following Hamiltonian with position-dependent spin-orbit coupling:

$$H = \frac{\hbar^2}{2m}[kI - A(r)]^2 + V(r), \quad (1)$$

where $A$ is a position-space vector of $2 \times 2$ matrices in the spin space, $V$ is a spin-space matrix, and $I$ is the identity matrix. For concreteness and simplicity we consider (pseudo)spin-1/2 atoms, i.e., systems with two dispersion branches. Generalization to higher-spin systems with more than two dispersion branches is straightforward and does not change the qualitative picture. Note that $A$ and $V$ may depend on position $r$ [51]. Wave vector $k$ and position $r$ are (noncommuting) operators. We separate the spin-dependent part of the potential,

$$V(r) = \sum_j v^j(r)\sigma^j + v_0(r)I, \quad (2)$$

and also make the spin dependence of the vector potential $A$ explicit,

$$A_j(r) = \sum_l a_j^l(r)\sigma^l, \quad (3)$$

where $\sigma^j$ are the Pauli matrices. Note that the square of the $A$ matrix is proportional to the identity matrix. We write position-space vectors using bold font and their indices as subscripts, whereas spin-space vectors are denoted by an arrow above and their indices are written as superscripts. The matrix $A$ may also contain a term proportional to the identity matrix. Such a term would describe the usual $U(1)$ electromagnetic field, which is beyond the scope of this paper, and we thus neglect it.

Using the matrices given in Eqs. (2) and (3), the Hamiltonian in Eq. (1) becomes

$$H = \frac{\hbar^2}{2m}I\sum_i k_i k_i + \sum_j \left(-\frac{\hbar^2}{2m}\sum_i \{k_i, a_i^j\} + v^j\right)\sigma^j + \left(\sum_{i,j}\frac{\hbar^2}{2m}a_i^j a_i^j + v_0\right)I, \quad (4)$$

where we have introduced the anticommutator $\{k_i, a_i^j\} = k_i a_i^j + a_i^j k_i$. The Hamiltonian above contains a term of the Zeeman form, and thus, it is natural to introduce the operator

$$B^j = -\frac{\hbar^2}{2m}\sum_i \{k_i, a_i^j\} + v^j, \quad (5)$$

which plays the role of the magnetic field in this term. We will therefore use the term "effective magnetic field" to describe the operator $B^j$ from here on. Furthermore, there is a spin-independent potential in the Hamiltonian,

$$W(r) = \frac{\hbar^2}{2m}\sum_{i,j}\left[a_i^j(r)\right]^2 + v_0(r). \quad (6)$$

We now are in the position to write down the initial Hamiltonian in the following concise manner:

$$H = \frac{\hbar^2}{2m}k^2 I + \vec{B}\cdot\vec{\sigma} + W(r)I \quad (7)$$

We proceed to look for the solution of the time-dependent Schrödinger equation

$$i\hbar\frac{\partial}{\partial t}\Psi = H\Psi \quad (8)$$

using adiabatic approximation by assuming that the distance between the eigenvalues of the operator $\vec{B}\cdot\vec{\sigma}$ is large compared to the off-diagonal terms.

## III. GENERAL EQUATIONS FOR ADIABATIC APPROXIMATION

In this section we treat the quantum-mechanical problem exactly first and then in the adiabatic approximation. We do not directly perform, for example, the expansion in orders of $\hbar$ as carried out in Refs. [45–49]. Instead, we postpone the semiclassical approximation to Sec. V.

### A. Unitary transformation

Anticipating adiabatic approximation, let us define a unitary operator $U$, which diagonalizes the term $\vec{B} \cdot \vec{\sigma}$ in spin space. Our problem is divided into two dispersion branches which we label with the sign of the eigenvalue of the operator $\vec{B} \cdot \vec{\sigma}$. In particular, the definition of $U$ implies that

$$\mathcal{P}_+^\dagger U^\dagger \vec{B} \cdot \vec{\sigma} U \mathcal{P}_- = \mathcal{P}_-^\dagger U^\dagger \vec{B} \cdot \vec{\sigma} U \mathcal{P}_+ = 0, \qquad (9)$$

where

$$\mathcal{P}_+ = \begin{pmatrix} 1 \\ 0 \end{pmatrix}, \quad \mathcal{P}_- = \begin{pmatrix} 0 \\ 1 \end{pmatrix} \qquad (10)$$

are the respective $\sigma^z$ eigenstates. Therefore, we can rewrite the diagonalized Zeeman term as

$$U^\dagger \vec{B} \cdot \vec{\sigma} U = \mathcal{P}_+^\dagger U^\dagger \vec{B} \cdot \vec{\sigma} U \mathcal{P}_+ + \mathcal{P}_-^\dagger U^\dagger \vec{B} \cdot \vec{\sigma} U \mathcal{P}_-. \quad (11)$$

The wave function in the diagonal basis is related to the original wave function by the same transformation,

$$\tilde{\Psi} = U^\dagger \Psi. \qquad (12)$$

Plugging this definition into Eq. (8) yields the Schrödinger equation in the new basis,

$$i\hbar \frac{\partial}{\partial t} \tilde{\Psi} = \tilde{H} \tilde{\Psi}, \qquad (13)$$

where from

$$\tilde{H} = U^\dagger H U \qquad (14)$$

we see that the Hamiltonian after the transformation retains its original form,

$$\tilde{H} = \frac{\hbar^2}{2m} \tilde{k}^2 I + \vec{\tilde{B}} \cdot \vec{\tilde{\sigma}} + W(\tilde{r}) I, \qquad (15)$$

and the effect of this transformation can be incorporated through a redefinition of the effective magnetic field, position, momentum, and spin operators, namely,

$$\tilde{r} = U^\dagger r U, \qquad (16a)$$

$$\tilde{k} = U^\dagger k U, \qquad (16b)$$

$$\vec{\tilde{\sigma}} = U^\dagger \vec{\sigma} U. \qquad (16c)$$

We note that although $\vec{\tilde{B}} \cdot \vec{\tilde{\sigma}}$ is proportional to $\sigma_z$, in general both $\vec{\tilde{B}}$ and $\vec{\tilde{\sigma}}$ have components in all three directions, and only their scalar product is diagonal in spin space.

### B. Adiabatic approximation

Thus far our discussion has been exact. Let us now perform adiabatic approximation by assuming that the wave function $\tilde{\Psi}$ remains in the eigenspace of the projection operator $\mathcal{P}_\pm \mathcal{P}_\pm^\dagger$, i.e., in either the lower or upper dispersion branch with respect to the position- and momentum-dependent effective magnetic field. Explicitly, $\tilde{\Psi} = \psi \mathcal{P}_\pm$ defines another wave function $\psi$, the components of which now evolve according to the Schrödinger equation with an effective Hamiltonian

$$H_{\text{eff}} = \mathcal{P}_\pm^\dagger \tilde{H} \mathcal{P}_\pm \qquad (17)$$

either in the lower $(-)$ or the upper $(+)$ branch. In the effective Hamiltonian the operators

$$r_{\text{c}} = \mathcal{P}_\pm^\dagger \tilde{r} \mathcal{P}_\pm = \mathcal{P}_\pm^\dagger U^\dagger r U \mathcal{P}_\pm, \qquad (18a)$$

$$k_{\text{c}} = \mathcal{P}_\pm^\dagger \tilde{k} \mathcal{P}_\pm = \mathcal{P}_\pm^\dagger U^\dagger k U \mathcal{P}_\pm \qquad (18b)$$

appear. They describe the position and momentum operators adiabatically projected to one of the branches. These operators $r_{\text{c}}$ and $k_{\text{c}}$ are sometimes called the covariant operators [45]. They are manifestly different from their canonical counterparts, signaling breakdown of the Galilean invariance [52]. Note that even though $r_{\text{c}}$ can be understood as a physical position operator (i.e., the position operator describing, e.g., the motion of the center of a wave packet), $k_{\text{c}}$ does not correspond to kinetic momentum. A kinetic momentum, also known as physical momentum [52], operator could be obtained by performing the transformations described here on $\hbar(kI - A)$, which is a matrix in spin space, as opposed to merely $\hbar k$. One can convince oneself that $\hbar(kI - A)$ is the kinetic momentum by computing the commutator between $r_{\text{c}}$ and the Hamiltonian in Eq. (1).

Since the position operator $r$ and the momentum operator $\hbar k$ are both spin independent, the projection operator commutes with them. Using this property, the last two equations can be rewritten as

$$r_{\text{c}} = r - \mathcal{A}^{(k)}, \qquad (19a)$$

$$k_{\text{c}} = k - \mathcal{A}^{(r)}, \qquad (19b)$$

where

$$\mathcal{A}^{(k)} = -\mathcal{P}_\pm^\dagger U^\dagger [r, U] \mathcal{P}_\pm, \qquad (20a)$$

$$\mathcal{A}^{(r)} = -\mathcal{P}_\pm^\dagger U^\dagger [k, U] \mathcal{P}_\pm. \qquad (20b)$$

Operators $\mathcal{A}^{(k)}$ and $\mathcal{A}^{(r)}$ represent the Berry connections. Given a suitable representation, commutators in these operators become derivatives, e.g., a commutator of a function in which the position operator is proportional to a momentum derivative in the momentum representation. Therefore, when the operator $U$ is diagonal in position or momentum basis, the Berry connection operator $\mathcal{A}^{(k)}$ or $\mathcal{A}^{(r)}$ becomes a connection in the usual geometric sense [see Eqs. (30) and (39)]. This also explains the seemingly counterintuitive labeling, which is standard [4].

In order to evaluate the potential term it is beneficial to expand $W(r)$ in a power series,

$$W(r) = w^{(0)} + \sum_j w_j^{(1)} r_j + \sum_{j,l} w_{jl}^{(2)} r_j r_l + \cdots . \qquad (21)$$

In most ultracold-atom-related problems the potential $W$ is, at most, quadratic, and we will therefore limit our attention to such cases. Cubic and higher-order terms in the potential $W$ would result in a more complicated expression in Eq. (24b). The effective Hamiltonian $H_{\text{eff}}$ can thus be rewritten in the following concise form:

$$H_{\text{eff}} = \frac{\hbar^2}{2m} k_{\text{c}}^2 + W(r_{\text{c}}) + \mathcal{V}, \qquad (22)$$

where

$$\mathcal{V} = \mathcal{P}_\pm^\dagger \vec{B} \cdot \vec{\sigma} \mathcal{P}_\pm + \mathcal{V}^{(r)} + \mathcal{V}^{(k)}, \tag{23}$$

with

$$\mathcal{V}^{(r)} = \frac{\hbar^2}{2m} (\mathcal{P}_\pm^\dagger U^\dagger [\boldsymbol{k}, U] \mathcal{P}_\mp) \cdot (\mathcal{P}_\mp^\dagger U^\dagger [\boldsymbol{k}, U] \mathcal{P}_\pm), \tag{24a}$$

$$\mathcal{V}^{(k)} = \sum_{j,l} w_{jl}^{(2)} \mathcal{P}_\pm^\dagger U^\dagger [r_j, U] \mathcal{P}_\mp \mathcal{P}_\mp^\dagger U^\dagger [r_l, U] \mathcal{P}_\pm. \tag{24b}$$

We see that besides the alternation of the physical momentum and position operators, three extra potential terms have appeared. In the following sections we investigate dynamics in this system in more detail.

### C. Heisenberg equations

As discussed above, the operators $\boldsymbol{r}_c$ and $\hbar \boldsymbol{k}_c$ do not represent the canonical position and momentum. This is confirmed by the observation that their commutators differ from the usual commutators for the position and momentum operators. In particular, not only does the position-momentum commutator gain an extra term, but the other commutators do not vanish anymore:

$$[(r_c)_j, (r_c)_l] = i\Theta_{jl}^{(k,k)}, \tag{25a}$$

$$[(k_c)_j, (k_c)_l] = i\Theta_{jl}^{(r,r)}, \tag{25b}$$

$$[(r_c)_j, (k_c)_l] = i\delta_{j,l} + i\Theta_{jl}^{(k,r)}, \tag{25c}$$

where various Berry curvatures are given by

$$\Theta_{jl}^{(k,k)} = i[r_j, \mathcal{A}_l^{(k)}] - i[r_l, \mathcal{A}_j^{(k)}], \tag{26a}$$

$$\Theta_{jl}^{(r,r)} = i[k_j, \mathcal{A}_l^{(r)}] - i[k_l, \mathcal{A}_j^{(r)}], \tag{26b}$$

$$\Theta_{jl}^{(k,r)} = i[r_j, \mathcal{A}_l^{(r)}] - i[k_l, \mathcal{A}_j^{(k)}], \tag{26c}$$

$$\Theta_{jl}^{(r,k)} = i[k_j, \mathcal{A}_l^{(k)}] - i[r_l, \mathcal{A}_j^{(r)}]. \tag{26d}$$

Also, note that $\Theta_{jl}^{(k,r)} = -\Theta_{lj}^{(r,k)}$. The emergence of the extra terms in Eqs. (25) can be interpreted as curving up of position space, momentum space, and phase space, respectively. In quantum mechanics phase space is inherently curved, as position and momentum operators do not commute to begin with. Equations (25) demonstrate that noncommutative geometry underlies the algebraic structure of coordinates and momenta. Noncommutative coordinates in the context of field theory, and physics in general, have attracted a great deal of theoretical interest [53,54].

Adiabatic approximation, and spin projection in particular, is essential to obtaining a nonzero Berry curvature (see Ref. [5] for an extensive discussion). If no spin projection is performed, Berry connections generally have a nontrivial matrix structure. Schematically, this matrix structure serves to generate terms of the $[\mathcal{A}, \mathcal{A}]$ type, which exactly cancel the corresponding $[k, \mathcal{A}]$ and $[r, \mathcal{A}]$ terms. In this way it is ensured that a change of basis in spin space leaves physical dynamics unchanged. On the other hand, adiabatic approximation confines evolution of the system to only one of the two dispersion branches, and

the price for that simplification is the emergence of Berry curvature.

Going beyond adiabatic approximation would bring about effects similar to *Zitterbewegung* (see Refs. [55–57]). In that case, noncommuting components of the velocity operator $\dot{\boldsymbol{r}}_c$ signal interbranch transitions. The frequency of these transitions is given by the gap between the dispersion branches.

Naturally, modified commutation relations result in altered Heisenberg equations for the covariant operators

$$\dot{\boldsymbol{k}}_c = \frac{1}{i\hbar} [\boldsymbol{k}_c, H_{\text{eff}}], \tag{27a}$$

$$\dot{\boldsymbol{r}}_c = \frac{1}{i\hbar} [\boldsymbol{r}_c, H_{\text{eff}}], \tag{27b}$$

which now contain the Berry curvature terms defined above,

$$\dot{\boldsymbol{k}}_c = -\frac{1}{\hbar} \nabla W(\boldsymbol{r}_c) + \frac{1}{i\hbar} [\boldsymbol{k}_c, \mathcal{V}]$$
$$+ \frac{\hbar}{2m} \sum_{j,l} \boldsymbol{e}_j \{\Theta_{jl}^{(r,r)}, (k_c)_l\}$$
$$+ \frac{1}{2\hbar} \sum_{j,l} \boldsymbol{e}_j \{\Theta_{jl}^{(r,k)}, \nabla_l W(\boldsymbol{r}_c)\}, \tag{28a}$$

$$\dot{\boldsymbol{r}}_c = \frac{\hbar}{m} \boldsymbol{k}_c + \frac{1}{i\hbar} [\boldsymbol{r}_c, \mathcal{V}]$$
$$+ \frac{\hbar}{2m} \sum_{j,l} \boldsymbol{e}_j \{\Theta_{jl}^{(k,r)}, (k_c)_l\}$$
$$+ \frac{1}{2\hbar} \sum_{j,l} \boldsymbol{e}_j \{\Theta_{jl}^{(k,k)}, \nabla_l W(\boldsymbol{r}_c)\}, \tag{28b}$$

where $\boldsymbol{e}_j$ denotes the unit vector in the $j$ direction (i.e., $\boldsymbol{e}_j$ is a vector, not a component of a vector), while all the $\nabla$'s here act on functions of a single variable and thus represent derivatives with respect to that variable. This set of Eqs. (28) represents the first main result of the paper.

The first term on the right-hand side in each of the two equations denotes the usual contribution known from classical mechanics, whereas the subsequent terms are due to adiabatic approximation. In particular, in each case the second term is due to emergent potentials, whereas the last two terms are due to Berry curvatures. In order to make our hitherto abstract discussion more concrete, we consider two simple examples next.

### IV. PARTICULAR CASES

Let us consider the situation where the operator $\vec{B}$ becomes a vector of complex numbers (as opposed to operators) in some representation. In this case the eigenvalues of the operator $\vec{B} \cdot \vec{\sigma}$ are $\pm|\vec{B}|$ with the eigenfunctions

$$\chi_+ = \begin{pmatrix} e^{-i\frac{\phi}{2}} \cos\frac{\alpha}{2} \\ e^{i\frac{\phi}{2}} \sin\frac{\alpha}{2} \end{pmatrix}, \quad \chi_- = \begin{pmatrix} e^{-i\frac{\phi}{2}} \sin\frac{\alpha}{2} \\ -e^{i\frac{\phi}{2}} \cos\frac{\alpha}{2} \end{pmatrix}, \tag{29}$$

where the spherical angles $\alpha$ and $\phi$ give the direction of the vector $\vec{B}$. The unitary operator $U$, which diagonalizes the matrix $\vec{B} \cdot \vec{\sigma}$, then consists of two columns, $\chi_+$ and $\chi_-$. Two

particular cases, which often occur in practice, are a position-dependent effective magnetic field and spin-orbit coupling, which corresponds to a momentum-dependent Zeeman term. We investigate them in more detail below.

### A. Position-space curvature

When the operator $\vec{B}$ depends only on the coordinate $\boldsymbol{r}$, the unitary transformation operator is a function of only position: $U = U(\boldsymbol{r})$. In this case the Berry connections are $\mathcal{A}^{(k)} = 0$ and

$$\mathcal{A}^{(r)} = i\chi_{\pm}^{\dagger}(\boldsymbol{r})\nabla^{(r)}\chi_{\pm}(\boldsymbol{r}). \tag{30}$$

The corresponding Berry curvatures are $\Theta^{(k,k)} = \Theta^{(k,r)} = \Theta^{(r,k)} = 0$ and

$$\Theta_{jl}^{(r,r)} = \nabla_j^{(r)}\mathcal{A}_l^{(r)} - \nabla_l^{(r)}\mathcal{A}_j^{(r)}. \tag{31}$$

The scalar potentials are $\mathcal{V}^{(k)} = 0$ and

$$\mathcal{V}^{(r)} = -\frac{\hbar^2}{2m}(\chi_{\pm}^{\dagger}\nabla^{(r)}\chi_{\mp})\cdot(\chi_{\mp}^{\dagger}\nabla^{(r)}\chi_{\pm}). \tag{32}$$

These quantities can also be expressed in terms of the angles on the Bloch sphere, namely, $\alpha$ and $\phi$. Concretely, the Berry connection is

$$\mathcal{A}^{(r)} = \pm\frac{1}{2}\cos\alpha\nabla^{(r)}\phi, \tag{33}$$

and the potential is the same for the two branches,

$$\mathcal{V}^{(r)} = \frac{\hbar^2}{8m}[(\nabla^{(r)}\alpha)^2 + \sin^2\alpha(\nabla^{(r)}\phi)^2], \tag{34}$$

while the Berry curvature is opposite for the two branches,

$$\Theta_{jl}^{(r,r)} = \pm\frac{\sin\alpha}{2}\big[\big(\nabla_j^{(r)}\phi\big)\big(\nabla_l^{(r)}\alpha\big) \\ - \big(\nabla_j^{(r)}\alpha\big)\big(\nabla_l^{(r)}\phi\big)\big]. \tag{35}$$

The latter two equations can also be conveniently expressed using the unit vector $\vec{n} = \vec{B}/|\vec{B}|$, describing the direction of the vector $\vec{B}$ [58],

$$\mathcal{V}^{(r)} = \frac{\hbar^2}{8m}(\nabla^{(r)}\vec{n})^2, \tag{36}$$

$$\Theta_{jl}^{(r,r)} = \mp\frac{1}{2}\vec{n}\cdot\big(\nabla_j^{(r)}\vec{n}\times\nabla_l^{(r)}\vec{n}\big). \tag{37}$$

The equations of motion (28) in this case are

$$\dot{\boldsymbol{k}}_{\mathrm{c}} = -\frac{1}{\hbar}\nabla^{(r)}W(\boldsymbol{r}_{\mathrm{c}}) + \frac{1}{i\hbar}[\boldsymbol{k}_{\mathrm{c}},\mathcal{V}] \\ + \frac{\hbar}{2m}\sum_{j,l}\boldsymbol{e}_j\big\{\Theta_{jl}^{(r,r)},(k_{\mathrm{c}})_l\big\}, \tag{38a}$$

$$\dot{\boldsymbol{r}}_{\mathrm{c}} = \frac{\hbar}{m}\boldsymbol{k}_{\mathrm{c}}. \tag{38b}$$

The curvature $\Theta_{jl}^{(r,r)}$ is also known as the synthetic magnetic field and has been studied theoretically [10,12] as well as experimentally [59,60]. Note that the Stern-Gerlach experiment [61], which is often discussed in introductory quantum mechanics textbooks [62], can also be described in this framework. In particular, a linear magnetic field

gradient separates out the two spin components since the Berry connection in position space becomes nonzero, even though the Berry curvature itself vanishes in that case.

### B. Momentum-space curvature

When operator $\vec{B}$ depends only on momentum $\boldsymbol{k}$, basis transformation is facilitated by $U = U(\boldsymbol{k})$, which then is a function of only momentum. In this case, the position-space Berry connection vanishes, $\mathcal{A}^{(r)} = 0$, whereas

$$\mathcal{A}^{(k)} = -i\chi_{\pm}^{\dagger}\nabla^{(k)}\chi_{\pm}. \tag{39}$$

Accordingly, the Berry-curvature components related to position space vanish, $\Theta^{(r,r)} = \Theta^{(k,r)} = \Theta^{(r,k)} = 0$, and all the curvature is concentrated in the momentum space,

$$\Theta_{jl}^{(k,k)} = -\nabla_j^{(k)}\mathcal{A}_l^{(k)} + \nabla_l^{(k)}\mathcal{A}_j^{(k)}. \tag{40}$$

The scalar potential has only momentum components, i.e., $\mathcal{V}^{(r)} = 0$ and

$$\mathcal{V}^{(k)} = -\sum_{j,l}w_{jl}^{(2)}\big(\chi_{\pm}^{\dagger}\nabla_j^{(k)}\chi_{\mp}\big)\big(\chi_{\mp}^{\dagger}\nabla_l^{(k)}\chi_{\pm}\big). \tag{41}$$

Equations similar to Eqs. (34)–(37) can also be written down in the case at hand. Finally, Heisenberg equations of motion (28) in this case are

$$\dot{\boldsymbol{k}}_{\mathrm{c}} = -\frac{1}{\hbar}\nabla^{(r)}W(\boldsymbol{r}_{\mathrm{c}}), \tag{42a}$$

$$\dot{\boldsymbol{r}}_{\mathrm{c}} = \frac{\hbar}{m}\boldsymbol{k}_{\mathrm{c}} + \frac{1}{i\hbar}[\boldsymbol{r}_{\mathrm{c}},\mathcal{V}] \\ + \frac{1}{2\hbar}\sum_{j,l}\boldsymbol{e}_j\big\{\Theta_{jl}^{(k,k)},\nabla_l^{(r)}W(\boldsymbol{r}_{\mathrm{c}})\big\}. \tag{42b}$$

We remark that, strictly speaking, when the two dispersion branches touch, adiabatic approximation becomes invalid. The condition for the validity of adiabatic approximation is particularly elegant in this momentum-space curvature case. Concretely, $|\vec{B}|$ must be nonzero for each $\boldsymbol{k}$. This is the case only when the system of equations

$$-\frac{\hbar^2}{m}\sum_i k_i a_i^j + v^j = 0 \tag{43}$$

has no solutions. In terms of $\boldsymbol{k}$, this system of equations is linear. Therefore, the branches do not touch only if the following determinant in spin space vanishes:

$$\sum_{j,l,n}\epsilon^{jln}a_1^j a_2^l a_3^n = 0, \tag{44}$$

where $\epsilon^{jln}$ is the Levi-Civita symbol. Effects of the momentum-space curvature have already been extensively studied theoretically [63,64].

### V. SEMICLASSICAL APPROXIMATION

As we saw in the last section, in cases where all the Berry curvature is concentrated in a single component, for example, as either position-space curvature or momentum-space curvature, the equations of motion are relatively simple and can often be treated exactly. However, this is not the case

in general. Moreover, in the definition of the Berry connection or the Berry curvatures, $\hbar$ is crucially absent, suggesting that these quantities also affect semiclassical dynamics. Finally, semiclassical approximation is of practical interest, as it allows one to investigate the motion of wave packets and clouds of ultracold atoms in particular. Motivated by these points, we consider semiclassical approximation in general in this section and proceed to apply it to particular Hamiltonians subsequently.

In semiclassical approximation we neglect the commutator between position and momentum. In that case the effective magnetic field operator becomes

$$B^j = -\frac{\hbar^2}{m} \sum_i k_i a_i^j(\boldsymbol{r}) + v^j(\boldsymbol{r}). \tag{45}$$

The matrix $\vec{B} \cdot \vec{\sigma}$ still has the eigenvectors $\chi_\pm$, but they now parametrically depend on the numbers $\boldsymbol{r}$ and $\boldsymbol{k}$. Berry connections (20) are

$$\mathcal{A}^{(r)} = i\chi_\pm^\dagger \nabla^{(r)} \chi_\pm, \tag{46a}$$

$$\mathcal{A}^{(k)} = -i\chi_\pm^\dagger \nabla^{(k)} \chi_\pm \tag{46b}$$

and lead to corresponding Berry curvatures (26),

$$\Theta_{jl}^{(k,k)} = -\nabla_j^{(k)} \mathcal{A}_l^{(k)} + \nabla_l^{(k)} \mathcal{A}_j^{(k)}, \tag{47a}$$

$$\Theta_{jl}^{(r,r)} = \nabla_j^{(r)} \mathcal{A}_l^{(r)} - \nabla_l^{(r)} \mathcal{A}_j^{(r)}, \tag{47b}$$

$$\Theta_{jl}^{(k,r)} = -\nabla_j^{(k)} \mathcal{A}_l^{(k)} - \nabla_l^{(r)} \mathcal{A}_j^{(r)}, \tag{47c}$$

$$\Theta_{jl}^{(r,k)} = \nabla_j^{(r)} \mathcal{A}_l^{(r)} + \nabla_l^{(k)} \mathcal{A}_j^{(k)}, \tag{47d}$$

and scalar potentials (24),

$$\mathcal{V}^{(r)} = -\frac{\hbar^2}{2m}(\chi_\pm^\dagger \nabla^{(r)} \chi_\mp) \cdot (\chi_\mp^\dagger \nabla^{(r)} \chi_\pm), \tag{48a}$$

$$\mathcal{V}^{(k)} = -\sum_{j,l} w_{jl}^{(2)} \chi_\pm^\dagger \nabla_j^{(k)} \chi_\mp \chi_\mp^\dagger \nabla_l^{(k)} \chi_\pm. \tag{48b}$$

Equations of motion (28) then take the form

$$\dot{\boldsymbol{k}}_c = -\frac{1}{\hbar} \nabla^{(r)} W - \frac{1}{\hbar} \nabla^{(r)} \mathcal{V}$$
$$+ \frac{\hbar}{m} \sum_{j,l} \boldsymbol{e}_j \Theta_{jl}^{(r,r)} (k_c)_l$$
$$+ \frac{1}{\hbar} \sum_{j,l} \boldsymbol{e}_j \Theta_{jl}^{(r,k)} \nabla_l^{(r)} W, \tag{49a}$$

$$\dot{\boldsymbol{r}}_c = \frac{\hbar}{m} \boldsymbol{k}_c + \frac{1}{\hbar} \nabla^{(k)} \mathcal{V}$$
$$+ \frac{\hbar}{m} \sum_{j,l} \boldsymbol{e}_j \Theta_{jl}^{(k,r)} (k_c)_l$$
$$+ \frac{1}{\hbar} \sum_{j,l} \boldsymbol{e}_j \Theta_{jl}^{(k,k)} \nabla_l^{(r)} W. \tag{49b}$$

We see that in semiclassical approximation Berry curvatures $\Theta$ and scalar potentials $\mathcal{V}$ do not vanish and still show up in the equations of motion. However, since they involve derivatives of

the eigenvectors $\chi_\pm$, which vary at scales much larger than the other relevant length scales, e.g., the de Broglie wavelength, these quantities are not dominant. Therefore, it is a reasonable approximation to insert classical relations $\dot{\boldsymbol{k}}_c \approx -\nabla^{(r)} W/\hbar$ and $\dot{\boldsymbol{r}}_c \approx \hbar \boldsymbol{k}_c/m$ on the right-hand side of the equations of motion. In that case, we arrive at

$$\dot{\boldsymbol{k}}_c = -\frac{1}{\hbar} \nabla^{(r)}(W + \mathcal{V})$$
$$+ \sum_{j,l} \boldsymbol{e}_j \big[ \Theta_{jl}^{(r,r)} (\dot{r}_c)_l + \Theta_{lj}^{(k,r)} (\dot{k}_c)_l \big], \tag{50a}$$

$$\dot{\boldsymbol{r}}_c = \frac{\hbar}{m} \boldsymbol{k}_c + \frac{1}{\hbar} \nabla^{(k)} \mathcal{V}$$
$$- \sum_{j,l} \boldsymbol{e}_j \big[ \Theta_{lj}^{(r,k)} (\dot{r}_c)_l + \Theta_{jl}^{(k,k)} (\dot{k}_c)_l \big], \tag{50b}$$

where we have grouped the terms in order to facilitate comparison with Eqs. (2.19) in Ref. [43]. Even though the result is the same, we arrived at it purely within the Hamiltonian formalism. Furthermore, in our derivation we have shown that these equations constitute a special case of the semiclassical situation; namely, they are valid only when Berry curvatures are small.

## VI. ONE-DIMENSIONAL SPIRAL

Up to this point our discussion has been valid for an arbitrary number of spatial dimensions. Now we specialize to a single spatial dimension, where the effects of phase-space Berry curvature are nevertheless nontrivial, as phase space in this case is two-dimensional. In particular, as an application of the discussion above, in this section we investigate the dynamics described by the following one-dimensional Hamiltonian:

$$H = H_0 - FxI, \tag{51}$$

where the $-FxI$ term describes a spin-independent force (linear potential), while

$$H_0 = \frac{\hbar^2}{2m}(kI - a\sigma_3)^2$$
$$+ \frac{\hbar\Omega}{2}\left( \cos\frac{x}{\lambda} \sigma_1 + \sin\frac{x}{\lambda} \sigma_2 \right) \tag{52}$$

is an exactly solvable Hamiltonian with a constant spin-orbit-coupling term and a position-dependent Zeeman term. The spin-orbit coupling term is characterized by its constant strength $a$. The position-space Zeeman term constitutes a spiral with a constant magnitude $\Omega/2$ and a wavelength $\lambda$. Furthermore, it is convenient to introduce the wave number

$$\kappa = \frac{\Omega}{2a}\frac{m}{\hbar}, \tag{53}$$

which quantifies the relative strength of the position-space and momentum-space Zeeman terms. This Hamiltonian $H_0$ is well known: it has undergone extensive theoretical investigation (see Ref. [17] and references therein) and has also been realized experimentally [16].

### A. Exact solution

In this section we recap the exact diagonalization [17] of $H_0$. We begin by observing that the Zeeman term can be rewritten as

$$\cos(x/\lambda)\sigma_1 + \sin(x/\lambda)\sigma_2 = e^{-i\frac{x}{2\lambda}\sigma_3}\sigma_1 e^{i\frac{x}{2\lambda}\sigma_3}, \quad (54)$$

and hence, the coordinate dependence may be eliminated by performing a unitary transformation. Concretely, the wave function in the new basis is

$$\tilde{\Psi} = U^\dagger \Psi, \quad (55)$$

where

$$U = e^{-i\frac{x}{2\lambda}\sigma_3}. \quad (56)$$

We then obtain the transformed Hamiltonian

$$\tilde{H}_0 = U^\dagger H_0 U = \frac{\hbar^2}{2m}(k - k_0\sigma_3)^2 + \frac{\hbar\Omega}{2}\sigma_1, \quad (57)$$

where

$$k_0 = a + \frac{1}{2\lambda}. \quad (58)$$

The symbols in this Hamiltonian directly correspond to physical quantities in the experimental realization of the model [16,17]. In particular, given two lasers with small detuning from the Raman resonance, $k_0$ is the wave-vector difference of the lasers (recoil wave vector), and $E_R = \hbar^2 k_0^2/2m$ is the recoil energy. The intensity of the two lasers is represented by the Rabi frequency $\Omega$. The dispersion is thus given by

$$\frac{E}{\hbar^2/m} = \frac{k^2}{2} + \frac{k_0^2}{2} \pm \sqrt{(kk_0)^2 + \frac{\Omega^2}{4}\left(\frac{m}{\hbar}\right)^2} \quad (59)$$

in the lower $(-)$ and the upper $(+)$ branches. The upper branch has a single quadratic minimum, whereas the lower branch has one quadratic minimum when

$$\hbar\Omega > 4E_R \quad (60)$$

and two quadratic minima or one quartic minimum otherwise. As the gap between the two branches is governed by the ratio $\hbar\Omega/E_R$ and we are interested in the situation where the adiabatic approximation is applicable, we limit further discussion to the single-minimum regime given in Eq. (60). Expanding the dispersion around the minimum $k = 0$, we find that the effective mass $m_\pm^*$ in the two branches is given by

$$\frac{m}{m_\pm^*} = 1 \pm \frac{2k_0^2}{\Omega}\frac{\hbar}{m} \approx 1 \pm \frac{1}{\kappa}\left(a + \frac{1}{\lambda}\right), \quad (61)$$

respectively. The first equality applies in the limit $k \ll k_0$ of interest when computing the effective mass, whereas the second approximation holds in the semiclassical regime. Indeed, the smallness of $1/\lambda a$ and $1/\lambda \kappa$ defines the semiclassical regime, where all the gradients are small compared to the de Broglie wavelength. Namely, when the period of the spiral $\lambda$ in the position-space Zeeman term is large compared to the spin-orbit-coupling wave number $a$, we have $1/\lambda a \ll 1$. In combination with the single-minimum condition, this also implies $1/\lambda \kappa \ll 1$. Note further that one can transform back from the physical Hamiltonian $\tilde{H}_0$ in Eq. (57) to the original

Hamiltonian $H_0$, Eq. (52), with arbitrary $\lambda$ and $a$ as long as Eq. (58) is satisfied.

In order to investigate the dynamics of the full Hamiltonian $H$, the force term $-FxI$ may be added to the exact solution as a perturbation. In that case one concludes that in the presence of spin-orbit coupling, the two branches (effective spin components) respond to a force differently, as one of them accelerates faster than the other.

### B. Semiclassical solution

We now treat $H$ including the effect of the force $F$ explicitly and also carefully tracing the effects of Berry curvatures in this system. The full Zeeman term now is a position- and momentum-dependent matrix:

$$\vec{B} \cdot \vec{\sigma} = \frac{\hbar\Omega}{2}\left(\cos\frac{x}{\lambda}\sigma_1 + \sin\frac{x}{\lambda}\sigma_2\right) - \frac{\hbar^2}{m}ak\sigma_3. \quad (62)$$

As this term contains both position and momentum operators, it does not conform to either of the cases addressed in Sec. IV. We therefore have to resort to the semiclassical approach.

The direction of the vector $\vec{B}$ can be written in terms of the spherical angles $\alpha(k)$ and $\phi(x)$ as introduced in Eq. (29). In particular,

$$\tan\alpha = -\frac{\kappa}{k}, \quad (63a)$$

$$\phi = \frac{x}{\lambda}. \quad (63b)$$

The eigenvalues of the matrix $\vec{B} \cdot \vec{\sigma}$ are

$$\pm|\vec{B}| = \pm\frac{\hbar\Omega}{2\kappa}\sqrt{\kappa^2 + k^2}. \quad (64)$$

For adiabatic approximation to hold, it is sufficient that the gap between the two branches, $2|\vec{B}|$, is larger than all the other relevant energy scales. This condition in particular enforces the single-minimum condition (60). The Berry connections are $\mathcal{A}^{(k)} = 0$ and

$$\mathcal{A}^{(r)} = \mp\frac{k}{2\lambda\sqrt{\kappa^2 + k^2}} \quad (65)$$

in this case. Note that due to the nonvanishing $\mathcal{A}^{(r)}$ [see Eq. (19b)], the physical momentum differs from the canonical momentum,

$$k_c = k\left(1 \pm \frac{1}{2\lambda\sqrt{\kappa^2 + k^2}}\right). \quad (66)$$

Position and momentum spaces remain flat, $\Theta^{(k,k)} = \Theta^{(r,r)} = 0$, and only phase-space Berry curvature is nonzero and opposite for the two branches:

$$\Theta^{(k,r)} = -\Theta^{(r,k)} = \pm\frac{\kappa^2}{2\lambda(\kappa^2 + k^2)^{\frac{3}{2}}}. \quad (67)$$

The scalar potentials (23) are $\mathcal{V}^{(k)} = 0$ and

$$\mathcal{V}^{(r)} = \frac{\hbar^2}{8m\lambda^2}\frac{\kappa^2}{\kappa^2 + k^2}, \quad (68)$$

and thus, the full potential $\mathcal{V}$ is

$$\mathcal{V} = \pm \frac{\hbar\Omega}{2\kappa}\sqrt{\kappa^2 + k^2} + \frac{\hbar^2}{8m\lambda^2}\frac{\kappa^2}{\kappa^2 + k^2}. \qquad (69)$$

Semiclassical dynamics follows Eqs. (49),

$$\dot{k}_c = \frac{F}{\hbar}(1 - \Theta^{(r,k)}), \qquad (70a)$$

$$\dot{x}_c = \frac{\hbar}{m}k_c(1 + \Theta^{(k,r)}) + \frac{1}{\hbar}\nabla^{(k)}\mathcal{V}, \qquad (70b)$$

which in general are quite complicated.

However, for our semiclassical approach to be valid, we should keep only the lowest-order corrections in the small parameters $1/\lambda a$ and $1/\lambda\kappa$. Furthermore, in order to prevent the kinetic energy from causing sizable interbranch transitions, we limit ourselves to the $|k| \ll \kappa$ regime, where the adiabatic approximation holds. These approximations lead to

$$k_c \approx k\left(1 \pm \frac{1}{2\lambda\kappa}\right), \qquad (71a)$$

$$\Theta^{(r,k)} = -\Theta^{(k,r)} \approx \mp\frac{1}{2\lambda\kappa}, \qquad (71b)$$

$$\frac{1}{\hbar}\nabla^{(k)}\mathcal{V} \approx \pm\frac{k}{\kappa}\frac{\Omega}{2\kappa}. \qquad (71c)$$

Therefore, equations of motion in this limit are

$$\dot{k}_c = \frac{F}{\hbar}\left(1 \pm \frac{1}{2\lambda\kappa}\right), \qquad (72a)$$

$$\dot{x}_c = \frac{\hbar}{m}k_c\left(1 \pm \frac{1}{2\lambda\kappa} \pm \frac{a}{\kappa}\right), \qquad (72b)$$

and for the center-of-mass motion we obtain the following closed equation:

$$\ddot{x}_c = \frac{F}{m}\left[1 \pm \frac{1}{\kappa}\left(\frac{1}{\lambda} + a\right)\right]. \qquad (73)$$

From this equation one can read off the effective mass, which is then seen to match the one given in Eq. (61).

We conclude that the effective mass in this model in semiclassical approximation is correctly captured for both branches by the phase-space Berry curvature. The Berry-curvature result is compared with the bare mass and also with the exact solution in Fig. 2. Thus, the effective mass measurement is a direct probe of the phase-space Berry curvature in this system. Therefore, effective-mass measurements in Refs. [65,66] can be reinterpreted as the first measurements of phase-space Berry curvature in ultracold-atom systems. This conclusion is the second main result of the paper.

## VII. SUMMARY AND OUTLOOK

In summary, we have presented a derivation of equations of motion in the presence of position-space, momentum-space, and phase-space Berry curvatures. We have relied on only the Hamiltonian formalism, and we have clearly separated adiabatic approximation, semiclassical approximation, and
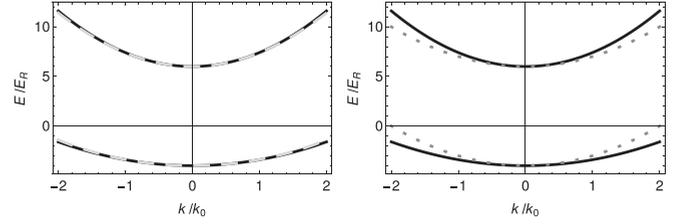


FIG. 2. Dispersion of the two branches in the units of the recoil energy $E_R$ and the recoil wave vector $k_0$ in the semiclassical single-minimum regime, $\hbar\Omega/E_R = 10$. The effective mass from the phase-space Berry curvature in Eq. (73) (solid line) is compared to the exact result (dashed line, left) and the bare-mass approximation $m_\pm^* = m$ (dotted line, right).

the low-curvature limit. Our approach has resulted in the Heisenberg equations of motion (28), which are written down with no reference to semiclassical approximation. From them, we have derived the semiclassical equations of motion (49). In the limit of small curvature they reduce to Eqs. (50). The latter can be directly compared to the results of Ref. [43]. Moreover, we have investigated the semiclassical dynamics in a system with an equal Rashba-Dresselhaus spin-orbit coupling system in a single spatial dimension. We have concluded that in the strong-coupling regime, where the dispersions of both branches are quadratic, the effective mass is directly related to phase-space Berry curvature.

Several directions of future work look promising. On the one hand, populating optical lattices with ultracold atoms, one can go far beyond the regimes readily achievable in solid-state physics. In particular, it possible to engineer strong artificial magnetic fields [30,31,67] as well as strong synthetic spin-orbit coupling [8,9,68], while motion of wave packets can be controlled and observed with remarkable precision [69–71]. This motivates one to generalize the presented approach and revisit the effects of phase-space Berry curvature on a lattice. Furthermore, in higher-dimensional models, the effects of phase-space Berry curvature most likely go beyond the rescaling of mass. In the one-dimensional system we have investigated, the phase space is two-dimensional, thus permitting only scalar curvature. In more dimensions, this is no longer true. Finally, in the semiclassical approach including the effects of harmonic confinement is straightforward, thus allowing one to consider trapped systems and analyze their collective modes.

[1] T. Frankel, *The Geometry of Physics: An Introduction* (Cambridge University Press, Cambridge, 2004).

[2] A. Einstein, Die Feldgleichungen der Gravitation, Sitzungsber. Preuss. Akad. Wiss. **25**, 844 (1915).

[3] C. N. Yang and R. L. Mills, Conservation of isotopic spin and isotopic gauge invariance, Phys. Rev. **96**, 191 (1954).

[4] D. Xiao, M.-C. Chang, and Q. Niu, Berry phase effects on electronic properties, Rev. Mod. Phys. **82**, 1959 (2010).

[5] T. Fujita, M. B. A. Jalil, S. G. Tan, and S. Murakami, Gauge fields in spintronics, J. Appl. Phys. **110**, 121301 (2011).

[6] A. Manchon, H. C. Koo, J. Nitta, S. M. Frolov, and R. A. Duine, New perspectives for Rashba spin-orbit coupling, Nat. Mater. **14**, 871 (2015).

[7] B. K. Stuhl, H.-I. Lu, L. M. Aycock, D. Genkina, and I. B. Spielman, Visualizing edge states with an atomic Bose gas in the quantum Hall regime, Science **349**, 1514 (2015).

[8] L. F. Livi, G. Cappellini, M. Diem, L. Franchi, C. Clivati, M. Frittelli, F. Levi, D. Calonico, J. Catani, M. Inguscio, and L. Fallani, Synthetic Dimensions and Spin-Orbit Coupling with an Optical Clock Transition, Phys. Rev. Lett. **117**, 220401 (2016).

[9] M. L. Wall, A. P. Koller, S. Li, X. Zhang, N. R. Cooper, J. Ye, and A. M. Rey, Synthetic Spin-Orbit Coupling in an Optical Lattice Clock, Phys. Rev. Lett. **116**, 035301 (2016).

[10] J. Dalibard, F. Gerbier, G. Juzeliūnas, and P. Öhberg, Colloquium: Artificial gauge potentials for neutral atoms, Rev. Mod. Phys. **83**, 1523 (2011).

[11] V. Galitski and I. B. Spielman, Spin-orbit coupling in quantum gases, Nature (London) **494**, 49 (2013).

[12] N. Goldman, G. Juzeliūnas, P. Öhberg, and I. B. Spielman, Light-induced gauge fields for ultracold atoms, Rep. Prog. Phys. **77**, 126401 (2014).

[13] H. Zhai, Degenerate quantum gases with spin-orbit coupling: A review, Rep. Prog. Phys. **78**, 026001 (2015).

[14] E. Rashba, Properties of semiconductors with an extremum loop. 1. Cyclotron and combinational resonance in a magnetic field perpendicular to the plane of the loop, Sov. Phys. Solid State **2**, 1109 (1960).

[15] G. Dresselhaus, Spin-Orbit Coupling Effects in Zinc Blende Structures, Phys. Rev. **100**, 580 (1955).

[16] Y.-J. Lin, K. Jiménez-García, and I. B. Spielman, Spin-orbit-coupled Bose-Einstein condensates, Nature (London) **471**, 83 (2011).

[17] Y. Li, G. I. Martone, and S. Stringari, Spin-orbit coupled Bose-Einstein condensates, in *Annual Review of Cold Atoms and Molecules* (World Scientific, Singapore, 2015), Chap. 5, p. 201.

[18] D. L. Campbell and I. B. Spielman, Rashba realization: Raman with RF, New J. Phys. **18**, 033035 (2016).

[19] L. Huang, Z. Meng, P. Wang, P. Peng, S.-L. Zhang, L. Chen, D. Li, Q. Zhou, and J. Zhang, Experimental realization of two-dimensional synthetic spin-orbit coupling in ultracold Fermi gases, Nat. Phys. **12**, 540 (2016).

[20] B. M. Anderson, G. Juzeliūnas, V. M. Galitski, and I. B. Spielman, Synthetic 3D Spin-Orbit Coupling, Phys. Rev. Lett. **108**, 235301 (2012).

[21] B. M. Anderson, I. B. Spielman, and G. Juzeliūnas, Magnetically Generated Spin-Orbit Coupling for Ultracold Atoms, Phys. Rev. Lett. **111**, 125301 (2013).

[22] T. Dubček, C. J. Kennedy, L. Lu, W. Ketterle, M. Soljačić, and H. Buljan, Weyl Points in Three-Dimensional Optical Lattices:

Synthetic Magnetic Monopoles in Momentum Space, Phys. Rev. Lett. **114**, 225301 (2015).

[23] J. Armaitis, J. Ruseckas, and G. Juzeliūnas, Omnidirectional spin Hall effect in a Weyl spin-orbit coupled atomic gas, Phys. Rev. A **95**, 033635 (2017).

[24] J. Struck, C. Ölschläger, M. Weinberg, P. Hauke, J. Simonet, A. Eckardt, M. Lewenstein, K. Sengstock, and P. Windpassinger, Tunable Gauge Potential for Neutral and Spinless Particles in Driven Optical Lattices, Phys. Rev. Lett. **108**, 225304 (2012).

[25] J. Struck, J. Simonet, and K. Sengstock, Spin-orbit coupling in periodically driven optical lattices, Phys. Rev. A **90**, 031601(R) (2014).

[26] A. Eckardt, Colloquium: Atomic quantum gases in periodically driven optical lattices, Rev. Mod. Phys. **89**, 011004 (2017).

[27] J. Struck, C. Ölschläger, R. L. Targat, P. Soltan-Panahi, A. Eckardt, M. Lewenstein, P. Windpassinger, and K. Sengstock, Quantum simulation of frustrated classical magnetism in triangular optical lattices, Science **333**, 996 (2011).

[28] M. Lewenstein, A. Sanpera, and V. Ahufinger, *Ultracold Atoms in Optical Lattices: Simulating Quantum Many-Body Systems* (Oxford University Press, Oxford, 2012).

[29] J. Struck, M. Weinberg, C. Ölschläger, P. Windpassinger, J. Simonet, K. Sengstock, R. Höppner, P. Hauke, A. Eckardt, M. Lewenstein, and L. Mathey, Engineering Ising-XY spin models in a triangular lattice via tunable artificial gauge fields, Nat. Phys. **9**, 738 (2013).

[30] M. Aidelsburger, M. Atala, M. Lohse, J. T. Barreiro, B. Paredes, and I. Bloch, Realization of the Hofstadter Hamiltonian with Ultracold Atoms in Optical Lattices, Phys. Rev. Lett. **111**, 185301 (2013).

[31] H. Miyake, G. A. Siviloglou, C. J. Kennedy, W. C. Burton, and W. Ketterle, Realizing the Harper Hamiltonian with Laser-Assisted Tunneling in Optical Lattices, Phys. Rev. Lett. **111**, 185302 (2013).

[32] N. Goldman, J. C. Budich, and P. Zoller, Topological quantum matter with ultracold gases in optical lattices, Nat. Phys. **12**, 639 (2016).

[33] A. Celi, P. Massignan, J. Ruseckas, N. Goldman, I. B. Spielman, G. Juzeliūnas, and M. Lewenstein, Synthetic Gauge Fields in Synthetic Dimensions, Phys. Rev. Lett. **112**, 043001 (2014).

[34] M. Mancini, G. Pagano, G. Cappellini, L. Livi, M. Rider, J. Catani, C. Sias, P. Zoller, M. Inguscio, M. Dalmonte, and L. Fallani, Observation of chiral edge states with neutral fermions in synthetic Hall ribbons, Science **349**, 1510 (2015).

[35] H. M. Price, O. Zilberberg, T. Ozawa, I. Carusotto, and N. Goldman, Four-Dimensional Quantum Hall Effect with Ultracold Atoms, Phys. Rev. Lett. **115**, 195303 (2015).

[36] D. Suszalski and J. Zakrzewski, Different lattice geometries with synthetic dimension, Phys. Rev. A **94**, 033602 (2016).

[37] E. Anisimovas, M. Račiūnas, C. Sträter, A. Eckardt, I. B. Spielman, and G. Juzeliūnas, Semisynthetic zigzag optical lattice for ultracold bosons, Phys. Rev. A **94**, 063632 (2016).

[38] M. V. Berry, Quantal phase factors accompanying adiabatic changes, Proc. R. Soc. London, Ser. A **392**, 45 (1984).

[39] F. Freimuth, R. Bamler, Y. Mokrousov, and A. Rosch, Phase-space Berry phases in chiral magnets: Dzyaloshinskii-Moriya interaction and the charge of skyrmions, Phys. Rev. B **88**, 214409 (2013).

[40] R. Bamler, Phase-Space Berry Phases in Chiral Magnets: Skyrmion Charge, Hall Effect, and Dynamics of Magnetic Skyrmions, Ph.D. thesis, University of Cologne, 2016 .

[41] C. Hanneken, F. Otte, A. Kubetzka, B. Dupé, N. Romming, K. Von Bergmann, R. Wiesendanger, and S. Heinze, Electrical detection of magnetic skyrmions by tunneling non-collinear magnetoresistance, Nat. Nanotechnol. **10**, 1039 (2015).

[42] K. Hamamoto, M. Ezawa, and N. Nagaosa, Purely electrical detection of a skyrmion in constricted geometry, Appl. Phys. Lett. **108**, 112401 (2016).

[43] G. Sundaram and Q. Niu, Wave-packet dynamics in slowly perturbed crystals: Gradient corrections and Berry-phase effects, Phys. Rev. B **59**, 14915 (1999).

[44] R. Shindou and K.-I. Imura, Noncommutative geometry and non-Abelian Berry phase in the wave-packet dynamics of Bloch electrons, Nucl. Phys. B **720**, 399 (2005).

[45] P. Gosselin, F. Ménas, A. Bérard, and H. Mohrbach, Semi-classical dynamics of electrons in magnetic Bloch bands: A Hamiltonian approach, Europhys. Lett. **76**, 651 (2006).

[46] P. Gosselin, A. Bérard, and H. Mohrbach, Semiclassical diag-onalization of quantum Hamiltonian and equations of motion with Berry phase corrections, Eur. Phys. J. B **58**, 137 (2007).

[47] P. Gosselin, H. Boumrar, and H. Mohrbach, Semiclassical quantization of electrons in magnetic fields: The generalized Peierls substitution, Europhys. Lett. **84**, 50002 (2008).

[48] P. Gosselin, J. Hanssen, and H. Mohrbach, Recursive diagonal-ization of quantum Hamiltonians to all orders in $\hbar$, Phys. Rev. D **77**, 085008 (2008).

[49] P. Gosselin and H. Mohrbach, Diagonal representation for a generic matrix valued quantum Hamiltonian, Eur. Phys. J. C **64**, 495 (2009).

[50] C. H. Wong and Y. Tserkovnyak, Quantum kinetic equation in phase-space textured multiband systems, Phys. Rev. B **84**, 115209 (2011).

[51] S.-W. Su, S.-C. Gou, I.-K. Liu, I. B. Spielman, L. Santos, A. Acus, A. Mekys, J. Ruseckas, and G. Juzeliūnas, Position-dependent spin-orbit coupling for ultracold atoms, New J. Phys. **17**, 033045 (2015).

[52] Y.-C. Zhang, Z.-Q. Yu, T. K. Ng, S. Zhang, L. Pitaevskii, and S. Stringari, Superfluid density of a spin-orbit-coupled Bose gas, Phys. Rev. A **94**, 033635 (2016).

[53] N. Seiberg and E. Witten, String theory and noncommutative geometry, J. High Energy Phys. **1999**, 032 (1999).

[54] M. R. Douglas and N. A. Nekrasov, Noncommutative field theory, Rev. Mod. Phys. **73**, 977 (2001).

[55] M. Merkl, F. E. Zimmer, G. Juzeliūnas, and P. Öhberg, Atomic Zitterbewegung, Europhys. Lett. **83**, 54002 (2008).

[56] L. J. LeBlanc, M. C. Beeler, K. Jimenez-Garcia, A. R. Perry, S. Sugawa, R. A. Williams, and I. B. Spielman, Direct observation of Zitterbewegung in a Bose-Einstein condensate, New. J. Phys. **15**, 073011 (2013).

[57] R. Winkler, U. Zülicke, and J. Bolte, Oscillatory multiband dynamics of free particles: The ubiquity of *zitterbewegung* effects, Phys. Rev. B **75**, 205314 (2007).

[58] G. E. Volovik, Linear momentum in ferromagnets, J. Phys. C **20**, L83 (1987).

[59] Y.-J. Lin, R. L. Compton, K. Jiménez-García, J. V. Porto, and I. B. Spielman, Synthetic magnetic fields for ultracold neutral atoms, Nature (London) **462**, 628 (2009).

[60] M. C. Beeler, R. A. Williams, K. Jimenez-Garcia, L. J. LeBlanc, A. R. Perry, and I. B. Spielman, The spin Hall effect in a quantum gas, Nature (London) **498**, 201 (2013).

[61] W. Gerlach and O. Stern, Der experimentelle Nachweis der Richtungsquantelung im Magnetfeld, Z. Phys. **9**, 349 (1922).

[62] J. J. Sakurai, *Modern Quantum Mechanics*, rev. ed. (Addison-Wesley, Reading, MA, 1994).

[63] H. M. Price, T. Ozawa, and I. Carusotto, Quantum Mechanics with a Momentum-Space Artificial Magnetic Field, Phys. Rev. Lett. **113**, 190403 (2014).

[64] H. M. Price, T. Ozawa, N. R. Cooper, and I. Carusotto, Artificial magnetic fields in momentum space in spin-orbit-coupled systems, Phys. Rev. A **91**, 033606 (2015).

[65] Y.-J. Lin, R. L. Compton, K. Jimenez-Garcia, W. D. Phillips, J. V. Porto, and I. B. Spielman, A synthetic electric force acting on neutral atoms, Nat. Phys. **7**, 531 (2011).

[66] J.-Y. Zhang, S.-C. Ji, Z. Chen, L. Zhang, Z.-D. Du, B. Yan, G.-S. Pan, B. Zhao, Y.-J. Deng, H. Zhai, S. Chen, and J.-W. Pan, Collective Dipole Oscillations of a Spin-Orbit Cou-pled Bose-Einstein Condensate, Phys. Rev. Lett. **109**, 115301 (2012).

[67] M. Aidelsburger, M. Lohse, C. Schweizer, M. Atala, J. T. Barreiro, S. Nascimbène, N. R. Cooper, I. Bloch, and N. Goldman, Measuring the Chern number of Hofstadter bands with ultracold bosonic atoms, Nat. Phys. **11**, 162 (2015).

[68] S. Kolkowitz, S. L. Bromley, T. Bothwell, M. L. Wall, G. E. Marti, A. P. Koller, X. Zhang, A. M. Rey, and J. Ye, Spin-orbit-coupled fermions in an optical lattice clock, Nature **542**, 66 (2017).

[69] A. Alberti, V. V. Ivanov, G. M. Tino, and G. Ferrari, Engi-neering the quantum transport of atomic wavefunctions over macroscopic distances, Nat. Phys. **5**, 547 (2009).

[70] A. Alberti, G. Ferrari, V. V. Ivanov, M. L. Chiofalo, and G. M. Tino, Atomic wave packets in amplitude-modulated vertical optical lattices, New J. Phys. **12**, 065037 (2010).

[71] E. Haller, R. Hart, M. J. Mark, J. G. Danzl, L. Reichsöllner, and H.-C. Nägerl, Inducing Transport in a Dissipation-Free Lattice with Super Bloch Oscillations, Phys. Rev. Lett. **104**, 200403 (2010).